Optical absorption of torus-shaped metal nanoparticles in the visible range

A. Mary
Departemento de Física Teórica de la Materia Condensada, Universitad Autónoma de Madrid, E-28049 Madrid, Spain

D. M. Koller, A. Hohenau, and J. R. Krenn
Institute of Physics and Erwin Schrödinger, Institute for Nanoscale Research, Karl-Franzens-University, Universitätsplatz 5, 8010 Graz, Austria

A. Bouhelier and A. Dereux
Institut Carnot de Bourgogne, CNRS-UMR 5209, Université de Bourgogne, F-21078 Dijon, France
(Received 22 November 2007; published 19 December 2007)

We theoretically and experimentally investigated the optical response of a thin metal nanotorus in the visible range. The close formulas describing the extinction cross sections of a torus are obtained in the nonretarded approximation. We demonstrate a good agreement between numerical simulations and experimental data. Our findings show that the main resonance is highly sensitive to the external medium and the geometrical parameters of the particle.

DOI: 10.1103/PhysRevB.76.245422 PACS number(s): 78.67.Bf, 73.20.Mf, 78.20.Ci

I. INTRODUCTION

The importance of localized surface plasmon in the optical properties of metallic nanoparticles is widely recognized.[1] Recent advances in fabrication techniques have spurred on intense research activities to understand and utilize metal resonances in various applications ranging from high-resolution near-field microscopy, negative refraction,[2] and sensors based on surface-enhanced Raman scattering.[3] Localized surface plasmons can be excited optically in a process that depends on size and geometry of the particle, as well as on the nature of the metal and the surrounding medium's dielectric functions.[4] Various shapes, such as rods,[5] disks,[6] shells,[7] rings,[8] and rices,[9] were investigated for their resolutely different characteristics. In this context, a recent study on the localized surface plasmon eigenmodes of metallic nanotorii theoretically demonstrated the existence of a nonzero magnetic dipole moment and a vanishing electric dipole moment at optical frequencies.[10] Due to the complexity of problem, the extinction cross section of a torus geometry was obtained either by time consuming calculations or by specifically dedicated numerical methods,[11] and close formulas are not available.

In this paper, we present the close formulas of the extinction cross sections of a small radius thin metal torus at optical frequencies. The derivation of the formulas is detailed in Sec. II. The analytical expressions, obtained in the nonretarded approximation, are analyzed and validated against numerical results for different torus thicknesses d and inner radius sizes R_{in} and are described in Sec. III. In addition, Sec. IV presents a comparison between our formulas and experimental extinction spectra obtained on arrays of small gold torii. A high tunability of the torus' plasmon resonances as a function of the ratio d/R_{in} is reported. We discuss the effects of the dielectric function of the embedding medium on plasmon resonance wavelengths in Sec. V. Finally, a summary is given in Sec. VI.

II. ANALYTICAL FORMULAS FOR EXTINCTION CROSS SECTIONS

The geometry studied in this work consists of an isolated subwavelength metal torus embedded in a dispersionless homogeneous external medium characterized by a dielectric function ϵ_1. The metal is described by the frequency dependent dielectric function $\epsilon(\omega)$. For the torus' dimensions considered here, the nonretarted approximation can be applied and Maxwell's equations can be reduced to a Laplace equation for the electric potential. This quantity can be expressed in toroidal coordinates, as shown in Fig. 1.[13] The relations between Cartesian coordinates x_1, x_2, x_3 (origin located at the center of gravity of the torus) and toroidal coordinates q_1, q_2, q_3 read[10]

$$q_1 = \operatorname{arctanh} \frac{2a\sqrt{x_1^2 + x_2^2}}{x_1^2 + x_2^2 + x_3^2 + a^2}, \tag{1}$$

$$q_2 = \arctan \frac{2ax_3}{x_1^2 + x_2^2 + x_3^2 - a^2}, \tag{2}$$

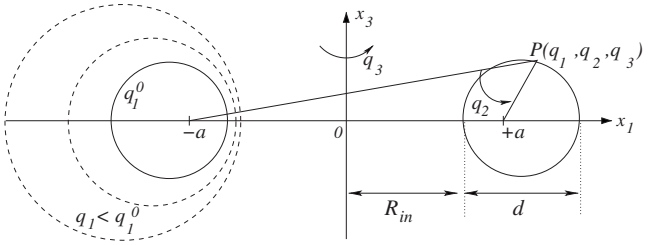

FIG. 1. Toroidal coordinate system where d defines the thickness and R_{in} the inner radius of the torus. A point P anywhere in space can be defined by q_1, q_2, q_3. The surface of the torus is defined by q_1^0.

$$q_3 = \arctan \frac{x_2}{x_1}, \tag{3}$$

where a is a constant such that $R_{in}+d/2=a \coth q_1$. A constant value of q_1 defines a circle of radius $a/\sinh(q_1)$ centered at $x_2=a \coth(q_1)$ and $x_3=0$. The coordinate q_3 is the azimuthal angle around the Cartesian axis x_3. A constant value $q_1=q_1^0$ defines the surface of a torus so that the volume of the torus is defined by $q_1>q_1^0$, while $q_1<q_1^0$ corresponds to the volume outside the torus. The torus aspect ratio d/R_{in} is given by $2\cosh(q_1^0-1)$.

In the nonretarded approximation, the incident electromagnetic field is modeled by a uniform electrostatic field of strength E_0. Two directions of polarization are relevant, either along the x_3 axis (axial polarization) or in the plane of the torus (for example, planar polarization along the x_1 axis). The associated electric potentials are $-E_0x_3$ and $-E_0x_1$, respectively. The planar polarization is experimentally important because it corresponds to an s- or p-polarized plane wave at normal incidence (i.e., incoming electric field points along the nanoparticle substrate). Consequently, we will only focus on a planar polarization in the following.

The coordinate x_1 is expanded in terms of toroidal harmonics (associated Legendre functions of the second kind) $Q^m_{n-1/2}(\cosh q_1)$,[10]

$$x_1 = -f\sum_{n=0}^{+\infty} \Delta_{n,0} Q^{m=1}_{n-1/2}(\cosh q_1)\cos(nq_2)\cos q_3, \tag{4}$$

where $f=\sqrt{\cosh q_1-\cos q_2}$ and $\Delta_{n,0}=2\sqrt{2}a(2-\delta_{n,0})/\pi$. For the sake of clarity and convenience, the abbreviation $Q^m_{n-1/2}(\cosh q_1)=Q^m_n$ will be used. This derivation relies on the thin torus assumption ($d<R_{in}$). The functions Q^1_n appearing in Eq. (4) can then be neglected for $n\geqslant 2$.[14,15] On the basis of the underlying symmetries of this approximation, the solutions of the Laplace equation inside and outside the torus are expanded as follows:

$$\Phi^{\text{in}}(\mathbf{r}) = f\sum_{n=0}^{1} D_n Q^1_n \cos(nq_2)\cos q_3, \tag{5}$$

$$\Phi^{\text{out}}(\mathbf{r}) = f\sum_{n=0}^{1} [A_n P^1_n + B_n Q^1_n]\cos(nq_2)\cos q_3, \tag{6}$$

where $P^m_{n-1/2}(\cosh q_1)=P^m_n$ is the associated Legendre functions of the first kind[10] and A_n, B_n, and D_n are constants fixed by boundary conditions. The condition for a uniform field far away of the torus combined with the asymptotic behavior of the functions P^m_n and Q^m_n imposes a constant value for all $B_n=-4\sqrt{2}naE_0/\pi$. From the continuity of the tangential components of the electric field at $q_1=q_1^0$, we find $D_n=A_nP^{m=1}_n(q_1=q_1^0)-B_n$. Rewriting in term of potential, the continuity of the normal component of the electric field displacement on the surface of the torus leads to a system of equations involving A_1 and A_2. The potential outside the torus can written as the sum of the applied potential and the potential of an electric dipole centered on the torus and aligned along x_1. This opens the possibility to derive a formula for the polarizability α_1 of the torus,

$$\alpha_1 = 4\pi v \frac{[\epsilon(\omega)-\epsilon_1]\eta_1 W_1}{C_0^1C_1^1-2G_0^1G_1^1}, \tag{7}$$

where v is the volume of the particle and η_1 is a dimensionless function of q_1^0. Its value is deduced from the matching of the electric dipole and the torus potentials. The functions G^m_n, C^m_n, and W_1 are defined by

$$G^m_n = \epsilon_1 Q^m_n(q_1^0) \left.\frac{dP^m_n}{dq_1}\right|_{q_1^0} - \epsilon(\omega) P^m_n(q_1^0) \left.\frac{dQ^m_n}{dq_1}\right|_{q_1^0}, \tag{8}$$

$$C^m_n = [\epsilon(\omega)-\epsilon_1]\sinh q_1^0 P^m_n(q_1^0)Q^m_n(q_1^0) - 2G^m_n \cosh q_1^0, \tag{9}$$

$$W_1 = \frac{2\sqrt{2}}{\pi}\left[\left.\frac{dQ^1_0}{dq_1}\right|_{q_1^0} \{C_1^1(2\cosh q_1^0 - \sinh q_1^0) + 2G_1^1\} + \left.\frac{dQ^1_1}{dq_1}\right|_{q_1^0} \{2G_1^1(2\cosh q_1^0 - \sinh q_1^0) + 2C_1^1\}\right], \tag{10}$$

where the abbreviations $Q^m_{n-1/2}(\cosh q_1^0)=Q^m_n(q_1^0)$ and $P^m_{n-1/2}(\cosh q_1^0)=P^m_n(q_1^0)$ are applied.

As the torus response is assimilated to the response of a dipole, the expression for the extinction cross section C_{ext} is obtained by the following relation:

$$C_{ext} = \frac{k^4}{6\pi}|\alpha_1|^2 + k\,\text{Im}\{\alpha_1\}. \tag{11}$$

Resonances in the extinction cross section are expected when the denominator in the expression of α_1 verifies,

$$C_0^1C_1^1 - 2G_0^1G_1^1 = 0. \tag{12}$$

This relation corresponds to the dispersion relation of an even surface plasmon eigenmode characterized by $M=1$, $N=0$. The quantum numbers M and N are related to the eigenmode symmetries over q_3 and q_2 axes, respectively. A comprehensive description of torus eigenmodes can be found in Ref. 10 and shows that the roots of Eq. (12) define two frequencies ω^- and ω^+.

Following a similar derivation, an analytical expression for the polarizability for an incident axial field is found,

$$\alpha_3 = 4\pi v \frac{[\epsilon(\omega)-\epsilon_1]\eta_3 W_3}{C_1^0C_2^0 - G_1^0G_2^0}, \tag{13}$$

where W_3 is defined as

$$W_3 = \frac{4\sqrt{2}}{\pi}\left[2\left.\frac{dQ^0_2}{dq_1}\right|_{q_1^0} \{G_2^0(2\cosh q_1^0 - \sinh q_1^0) + C_2^0\} - \left.\frac{dQ^0_1}{dq_1}\right|_{q_1^0} \{C_2^0(2\cosh q_1^0 - \sinh q_1^0) + G_2^0\}\right]. \tag{14}$$

The expression of polarizability reveals that the $M=0$,

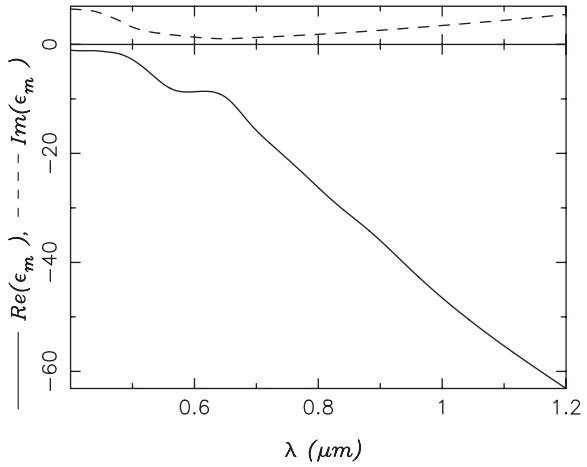

FIG. 2. Real part (solid line) and imaginary part (dashed line) of the dielectric function of gold compiled form Ref. 12.

$N=1$ odd eigenmode is excited when the corresponding dispersion relation is satisfied,

$$C_1^0 C_2^0 - G_1^0 G_2^0 = 0. \tag{15}$$

III. ANALYTICAL AND NUMERICAL RESULTS

Having in mind the stringent requirements for fabricating nanostructures, we will focus our analysis on gold torii. The complex dielectric function $\epsilon(\omega)$ of gold was compiled form experimental data[12] and is plotted in Fig. 2 for reference. Using the values of $\epsilon(\omega)$, we can now plot the extinction cross sections for three decreasing aspect ratios d/R_{in} labeled t_a, t_b, and t_c, as shown in Fig. 3(a). For this calculation, the dielectric constant of the external medium is constant to 1. The Legendre functions are calculated numerically by using the algorithm developed by Segura and Gil.[16]

The graph demonstrates that for an in-plane excitation field, the torus exhibits size-dependent surface plasmon resonances situated in the visible and near infrared region. Such behavior was also reported for gold nanorings[8] and nanoshells.[7] Using the expression of α_1, these resonance peaks can be attributed to the lower frequency ω^- of the $M=1$, $N=0$ torus surface plasmon eigenmode. Resonance peaks due to ω^+ are not visible due to the absorption inside metal. For the t_a spectrum, a second peak is visible at 580 nm. We attribute this feature to Au interband electronic transitions located between 550 and 620 nm (see Fig. 2). Figure 3(b) shows the t_a, t_b, and t_c extinction cross sections calculated for an axial excitation. To the difference with an in-plane excitation field, the resonance positions are only weak depending on the aspect ratio d/R_{in} of the torus.

To verify these analytical results, we performed numerical simulations of the extinction cross section. Maxwell's equations were solved by using the fully retarded Green's dyadic method in which the torus is discretized in small unit cells. The large number of unit cell is necessary to obtain convergent spectra. Extinction cross sections obtained by this numerical method are plotted in red in Fig. 3(a), and in Fig. 3(b), for a planar and axial excitation field, respectively. For both excitations, a good agreement is found between analytical and numerical extinction cross sections. In particular, the resonances centered around 498 nm for an axial illumination are independent of the aspect ratio. For an electric field polarized along the x_1 axis, the numerical simulations also exhibit the size-dependent plasmon resonance observed with the analytical derivation. For all the aspect ratios considered here, the peak positions and the absolute weights of the resonances are well reproduced by our analytical model. The heights of the peaks are lower in Green dyadic method, mainly due to the fact that torus is not ideally discretized. Nevertheless, these numerical calculations confirm the validity of our different approximations notably in the nonretarded case.

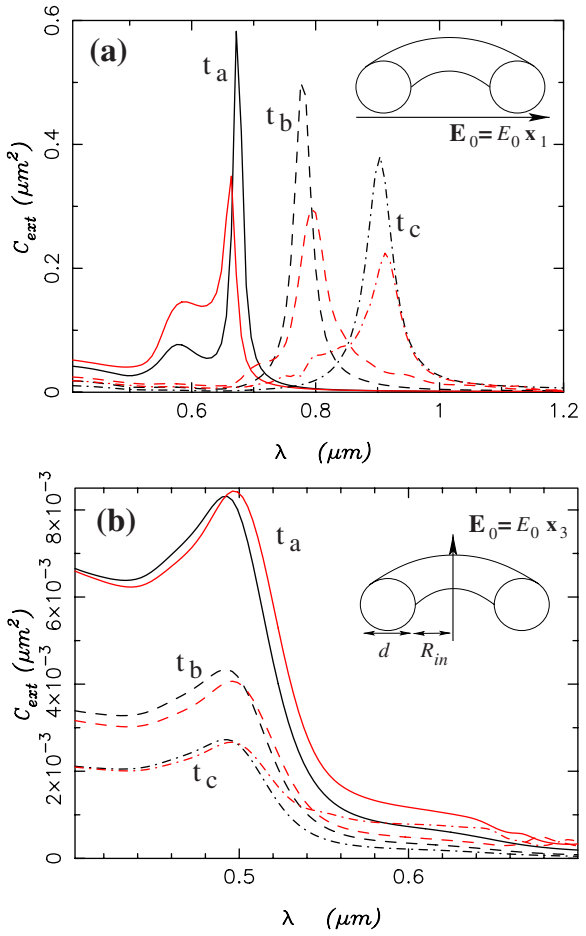

FIG. 3. (Color online) Extinction cross sections calculated by Eq. (11) (black curves) and by the dyadic Green method (red/gray curves) (a) for planar applied field and (b) for an axial applied field. Three different form ratios are considered: torus t_a, $d=21$ nm and $R_{in}=21$ nm ($d/R_{in}=1$); t_b, $d=15$ nm and $R_{in}=27$ nm ($d/R_{in}=0.55$); and t_c, $d=12$ nm and $R_{in}=30$ nm ($d/R_{in}=0.4$). The external medium is air.

IV. EXPERIMENTAL RESULTS

In order to compare our theoretical results with experimental data, arrays of Au nanorings were fabricated by

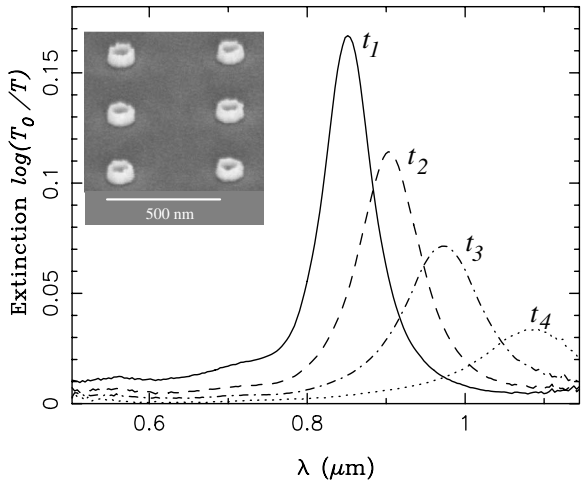

FIG. 4. Measured extinction spectra for different ratios of d/R_{in}: torus t_1, $d=31$ nm and $R_{in}=32$ nm ($d/R_{in}=0.97$); t_2, $d=28$ nm and $R_{in}=33$ nm ($d/R_{in}=0.85$); t_3, $d=25$ nm and $R_{in}=35$ nm ($d/R_{in}=0.71$); and t_4, $d=20$ nm and $R_{in}=40$ nm ($d/R_{in}=0.5$). The external medium is air. Inset: electron micrograph of gold nanorings prepared by electron-beam lithography. The period of the array is fixed to $\Gamma=500$ nm.

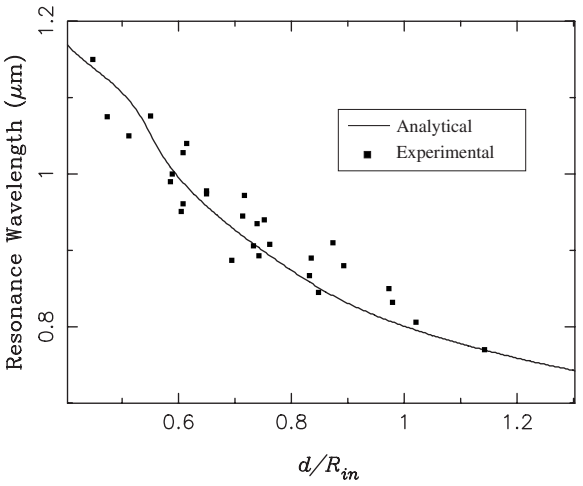

FIG. 5. Experimental (square dots) and analytical (solid line) resonance wavelengths versus d/R_{in} for an in-plane excitation field.

electron-beam lithography.[18] An electron micrograph of a typical sample is shown in the inset of Fig. 4. The period of the arrays ($\Gamma=500$ nm) is large enough to neglect near-field interactions between particles. The nanorings have external diameters ranging from 80 to 130 nm and a height of 50 nm. Optical properties of the Au nanorings were investigated by extinction spectroscopy [$ext=\log(T_0/T)$]. The samples are illuminated by an incident plane wave with its E-field vector oriented in the plane of particles. Measured spectra for different ratios of d/R_{in} are plotted in Fig. 4.

Optical spectra were measured for many samples presenting a large range of aspect ratio. The effect of the glass substrate is qualitatively incorporated in our analytical theory by considering that the torii are surrounded by a material with dielectric constant $\epsilon_1=2.12$. These theoretical results are compared to our experimental findings summarized in Fig. 5. The plot shows the position of the resonance wavelengths as a function of d/R_{in}. A good agreement is found for aspect ratios ranging between 0.4 and 1.2. In particular, the redshift of resonance wavelengths observed for increasing d/R_{in} is well reproduced by the $M=1$, $N=0$ eigenmode of the torus. We note that this particular eigenmode has the same properties as the symmetric $M=1$ mode of the ring reported in Ref. 8.

V. TUNABILITY OF THE TORUS PLASMON RESONANCES AS A FUNCTION OF THE EMBEDDING MEDIUM

Finally, we would like to address the question of the dependence of the resonance wavelength to the surrounding medium. Figure 6 shows the spectral position of the resonance versus the refractive index of the environment $n_1=\sqrt{\epsilon_1}$ for an in-plane electric field. We found a high sensitivity of the resonance to changes of the surrounding refractive index with a pronounced redshift of the peak for increasing values of n_1. This shift drastically depends on the aspect ratio of the torus with the largest shift observed for small d/R_{in}. A sensitivity of 444 nm and/or refractive index unit (RIU) is calculated for $d/R_{in}=1$. The sensitivity increases from 880 nm/RIU for $d/R_{in}=0.5$ to 1660 nm/RIU for $d/R_{in}=0.2$, the smallest aspect ratio considered here. This sensitivity is in agreement with experimental results obtained with Au nanorings.[17] We have also performed calculations for an axial excitation field (data not shown). Resonance wavelengths obtained in this case present a very low sensitivity to the nature of the surrounding medium (7 nm/RIU) which is independent on the aspect ratio.

VI. SUMMARY

In conclusion, we derived analytical expressions for the extinction cross sections of thin metal nanotorii, and we

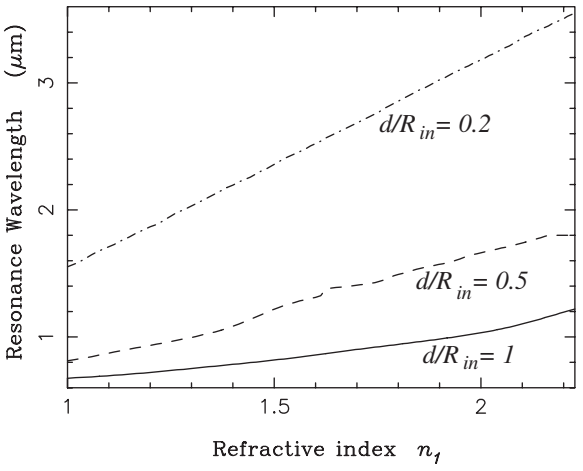

FIG. 6. Resonance wavelength for planar excitation field versus refractive index n_1. Three values of d/R_{in} are considered: 1, 0.5, and 0.2.

found a good agreement with Green's dyadic numerical calculations. Our numerical derivations are also in agreement with experimental data indicating the validity of our approach. The physical origin of the resonances is very similar to previously reported spectral response of ringlike particles. By changing the refractive index of the environment of the particles, we have shown a high sensitivity of the plasmon peaks to the external medium. The sensitivity can be modulated by changing the aspect ratio of the inner to outer diameters of the torus. The high sensitivity reported here suggests the potential utilization of gold nanotorus for ultrasensitive refractive index sensor applications.

ACKNOWLEDGMENTS

This work was supported by the Regional Council of Burgundy (ARCEN project) and by the European Commission (NoE Contract No. FP6-IST-2002-1-507879).

[1] U. Kreibig and M. Vollmer, *Optical Properties of Metal Clusters*, Springer Series in Material Sciences, Vol. 25 (Springer, Berlin, 1995).
[2] S. Linden, C. Enkrich, M. Wegener, J. Zhou, T. Koschny, and C. M. Soukoulis, Science **306**, 1351 (2004).
[3] K. Kneipp, Y. Wang, H. Kneipp, L. T. Perelman, I. Itzkan, R. R. Dasari, and M. S. Feld, Phys. Rev. Lett. **78**, 1667 (1997).
[4] J. Homola, S. S. Yee, and G. Gauglitz, Sens. Actuators B **54**, 3 (1999).
[5] N. R. Jana, L. Gearheart, and C. J. Murphy, J. Phys. Chem. B **105**, 4065 (2001).
[6] Y. Sun and Y. Xia, Science **298**, 2176 (2002).
[7] E. Prodan, C. Radloff, N. J. Halas, and P. Nordlander, Science **302**, 419 (2003).
[8] J. Aizpurua, P. Hanarp, D. S. Sutherland, M. Käll, G. W. Bryant, and F. J. Garcia de Abajo, Phys. Rev. Lett. **90**, 057401 (2003).
[9] H. Wang, D. W. Brandl, F. Le, P. Nordlander, and N. J. Halas, Nano Lett. **6**, 827 (2006).
[10] A. Mary, A. Dereux, and T. L. Ferrell, Phys. Rev. B **72**, 155426 (2005).
[11] F. J. Garcia de Abajo and A. Howie, Phys. Rev. B **65**, 115418 (2002).
[12] E. D. Palik, *Handbook of Optical Constants of Solids* (Academic, San Diego, CA, 1985).
[13] P. M. Morse and H. Feshbach, *Methods of Theoretical Physics* (Mc Graw-Hill, New York, 1953).
[14] J. A. Hernandes and A. K. T. Assis, Phys. Rev. E **68**, 046611 (2003).
[15] A. Mary, Ph.D. thesis, Université de Bourgogne, Dijon, 2006.
[16] J. Segura and A. Gil, Comput. Phys. Commun. **124**, 104 (2000).
[17] E. M. Larsson, J. Alegret, M. Kall, and D. S. Sutherland, Nano Lett. **7**, 1256 (2007).
[18] A. Hohenau, H. Ditlbacher, B. Lamprecht, J. R. Krenn, A. Leitner, and F. R. Aussenegg, Microelectron. Eng. **83**, 1464 (2006).